Annual Symposium of the Hellenic Nuclear Physics Society

Τόμ. 16 (2008)

HNPS2008

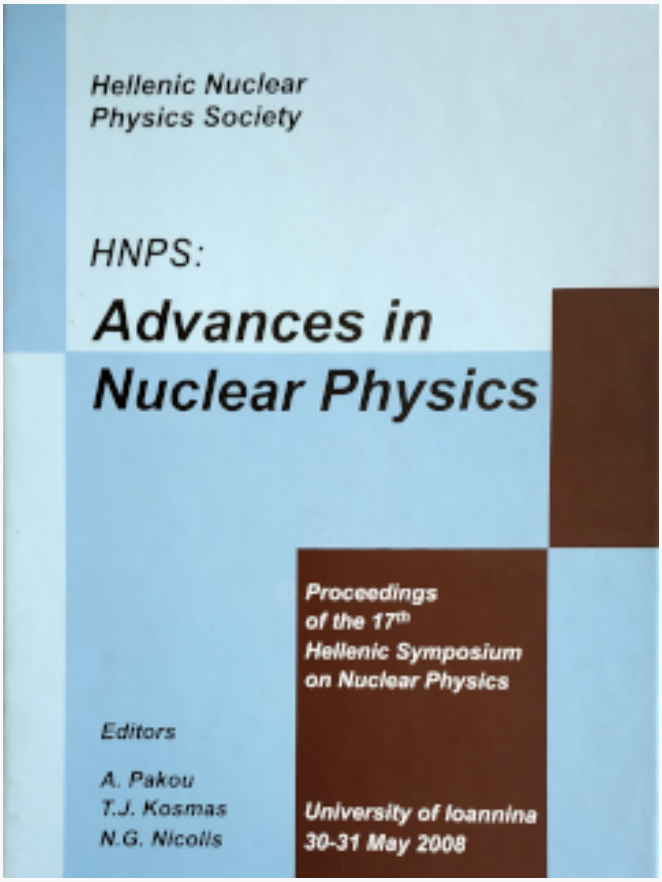

Microscopic description of nuclear quantum phase transitions

G. A. Lalazissis, T. Niksic, D. Vretenar, P. Ring

doi: 10.12681/hnps.2576

Microscopic description of nuclear quantum phase transitions

G. A. Lalazissis [a] T. Nikšić, [b] D. Vretenar [b] P. Ring [c]

[a] *Department of Theoretical Physics, Aristotle University of Thessaloniki, Thessaloniki Gr-54124, Greece*

[b] *Physics Department, Faculty of Science, University of Zagreb, 10000 Zagreb, Croatia*

[c] *Physik-Department der Technischen Universität München, D-85748 Garching, Germany*

Abstract

The relativistic mean-field framework, extended to include correlations related to restoration of broken symmetries and to fluctuations of the quadrupole deformation, is applied to a study of shape transitions in Nd isotopes. It is demonstrated that the microscopic self-consistent approach, based on global effective interactions, can describe not only general features of transitions between spherical and deformed nuclei, but also the singular properties of excitation spectra and transition rates at the critical point of quantum shape phase transition.

1 Introduction

Quantum phase transitions (QPT) between competing ground-state phases can be induced by variation of a non-thermal control parameter at zero temperature. In the case of atomic nuclei, in particular, first- and second-order QPT can occur between systems characterized by different ground-state shapes. Nuclear shape phase transitions have been the subject of a number of recent theoretical and experimental studies, pioneered by Iachello (1; 2), Casten and Zamfir (3; 4). These transitions can be described in the geometric framework in terms of a Bohr Hamiltonian for shape variables, and related to the concept of critical symmetries which provide parameter independent (up to overall scale factors) predictions for excitation spectra and electric quadrupole (E2) transition rates for nuclei at the phase transition point (1). Alternatively, in the approach of algebraic models the different shapes coincide with particular dynamic symmetries of some algebraic structure, and the phase transition

occurs when these symmetries are broken in a specific way (2; 5). In both approaches, geometric and algebraic, the description of QPT is based on model specific Hamiltonians which by construction describe shape changes. A shape phase transition is then accessed by variation of a control parameter. Analytic solutions of the eigenvalue problem at the critical point are associated with zeros of special functions, corresponding to a particular (critical) symmetry of the Hamiltonian.

In this work we address the important question whether nuclear QPT can also be described in a general microscopic framework, based on effective nucleon-nucleon interactions or universal energy density functionals, that provides a unified description of bulk properties (masses, density distributions, radii) and excitation spectra. In particular, properties of heavy nuclei with a large number of active valence nucleons are best described in the framework of self-consistent mean-field models. A variety of structure phenomena have been described with mean-field models based on the Gogny interaction, the Skyrme energy functional, and the relativistic meson-exchange effective Lagrangian (10; 11). The self-consistent mean-field approach to nuclear structure represents an approximate implementation of Kohn-Sham density functional theory, which enables a description of the nuclear many-body problem in terms of a universal energy density functional. Important advantages of the mean-field approach include the use of global effective nuclear interactions, the treatment of arbitrarily heavy systems, and the intuitive picture of intrinsic shapes.

2 Results and discussion

In several recent studies (12; 13; 14), the self-consistent mean-field framework has been employed in the calculation of potential energy curves (PECs) as functions of the quadrupole deformation, for a number of isotopic chains in which the occurrence of critical point symmetries had been predicted. The PECs calculated with a constraint on the mass quadrupole moment display shape transitions from spherical to deformed configurations. It was shown that particular isotopes exhibit relatively flat PECs over an extended range of the deformation parameter, and this has been interpreted as signature of certain types of critical point symmetries. A simple mean-field approach, however, cannot be used for a quantitative analysis of critical point nuclei. Flat PECs are one of the characteristics of critical point symmetries, but PECs alone do not single out a specific isotope as being the critical one. The concept of shape phase transition and related critical point symmetry includes analytic expressions for observables: excitation energies and transition rates. Thus in order to attribute a critical point symmetry to a specific nucleus, and to show that neighboring isotopes do not exhibit this symmetry, one must be able to calculate the ratios of excitation energies and B(E2) rates, and this is not

possible on the mean-field level. For a quantitative description of nuclei with soft potential energy surfaces it is necessary to explicitly consider correlation effects beyond the mean-field level: the restoration of rotational symmetry and fluctuations of the quadrupole deformation. This allows the calculation of spectra and transition rates, and therefore provides the basis for a quantitative prediction of shape transitions. In addition, in open-shell nuclei projection on particle number is crucial whenever the number of correlated pairs becomes small and the density of levels is low, a situation typical for the description of phenomena related to the evolution of shell structure. In order to single out the critical point isotope, it is thus necessary to perform the projection on eigenstates of the particle number operators.

In two recent articles (15; 16) we have developed a model which extends the relativistic self-consistent mean-field approach to include correlations related to restoration of broken symmetries and to fluctuations of collective variables. The model uses the generator coordinate method (GCM) to perform configuration mixing of angular-momentum and particle-number projected many-body wave functions, generated from the solutions of the relativistic mean-field + Lipkin-Nogami BCS equations, with a constraint on the mass quadrupole moment. A point-coupling nucleon-nucleon effective interaction is used in the particle-hole channel, and a density-independent δ-interaction in the pairing channel.

In the present study we apply this model to the description of shape transitions and address the following question: can a universal density functionals, with parameters adjusted to global ground-state properties (masses, radii) of nuclei over the whole mass table, at the same time reproduce the singular behavior of excitation spectra at the critical point of shape phase transition? In the current version our model is restricted to the description of axially symmetric shapes. We will thus consider transitions between spherical and axially deformed shapes in the chain of Nd isotopes. In the language of the interacting boson model this is a transition between U(5) and SU(3) dynamical symmetries, and in Ref. (2) it has been shown that along this path a first-order shape phase transition occurs, associated with the X(5) critical symmetry. An approximate solution in terms of zeros of Bessel functions of irrational order was presented for the particular case in which the β and γ degrees of freedom are decoupled and only the β-term is retained in the transition operator. Evidence for the empirical realization of X(5) critical symmetry was first reported for ^{152}Sm and other $N = 90$ isotones in Ref. (4). By comparing the experimental low-spin level scheme and reduced transition probabilities with parameter-free X(5) predictions, in Ref. (18) it has been shown that ^{150}Nd presents a very good case of X(5) critical symmetry. This symmetry has been studied in a number of recent papers, both in the geometric and algebraic approach and, in particular, the dynamics at the critical point of a general first-order quantum phase transition has been analyzed from an algebraic perspective

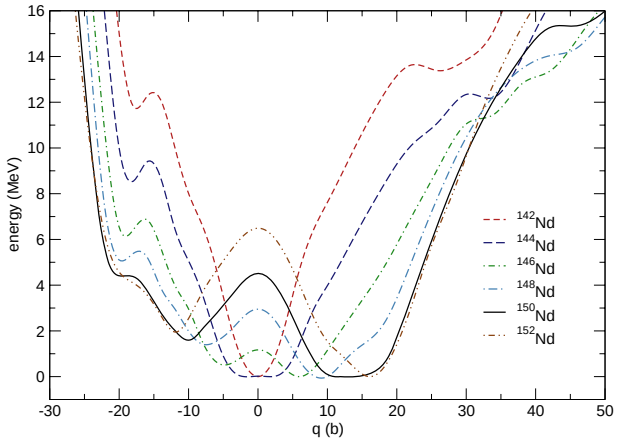

Fig. 1. Self-consistent relativistic mean-field plus Lipkin-Nogami BCS binding energy curves of $^{142-152}$Nd, as functions of the mass quadrupole moment.

in Ref. (19). An exactly separable γ-rigid version (with $\gamma = 0$) of the X(5) symmetry has recently been constructed (20), and denoted X(3).

In the following we report self-consistent GCM calculations based on the relativistic point-coupling effective interaction PC-F1 (21), which has been adjusted to ground-state observables (binding energies, charge radii, diffraction radii, surface thickness) of spherical nuclei, and tested in the analysis of the equation of state of symmetric nuclear matter and neutron matter, binding energies and form-factors, and ground-state properties of several isotopic and isotonic chains. In addition to the mean-field potential, pairing correlations are described in the Lipkin-Nogami (LN) BCS approximation. A density-independent δ-force is used as the effective interaction in the particle-particle channel. As explained in Ref. (16), the proton and neutron pairing strengths that were determined simultaneously with the PC-F1 parameters, have to be reduced by $\approx 10\%$ so that the projected average pairing gaps reproduce the BCS pairing gaps: $V_p = -260$ MeV and $V_n = -285$ MeV. Refs. (15; 16) include a detailed description of the model and the numerical implementation of the relativistic GCM with angular-momentum and particle-number projections.

For an axially deformed nucleus the energy surface as function of deformation is obtained by imposing a constraint on the mass quadrupole moment. The mean-field breaks rotational symmetry, and the particle number is only approximately restored by the Lipkin-Nogami procedure. In order to be able to compare model predictions with data, states with good angular momentum and particle number are projected from the mean-field + LN BCS solutions. For each value of the angular momentum the solution of the Hill-Wheller eigenvalue equations determines the excitation spectrum. In Fig. 1 we plot the self-consistent relativistic mean-field + LN BCS binding energy curves of $^{142-152}$Nd, as functions of the mass quadrupole moment. The PECs display a gradual transition between the spherical ^{142}Nd and strongly prolate deformed

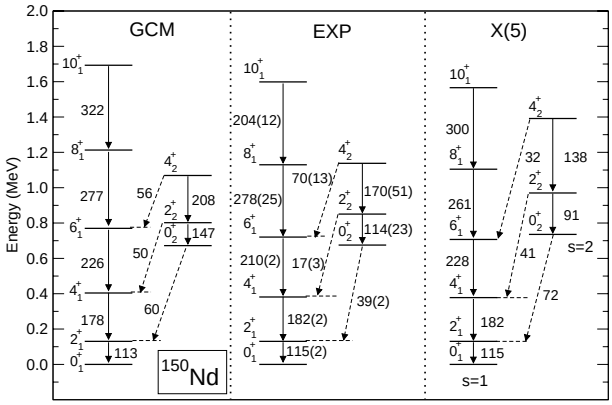

Fig. 2. The particle-number projected GCM spectrum of ^{150}Nd (left), compared with the data (18) (middle), and the X(5)-symmetry predictions (right) for the excitation energies, intraband and interband B(E2) values (in Weisskopf units) of the ground-state ($s = 1$) and β_1 ($s = 2$) bands. The theoretical spectra are normalized to the experimental energy of the state 2_1^+, and the X(5) transition strengths are normalized to t

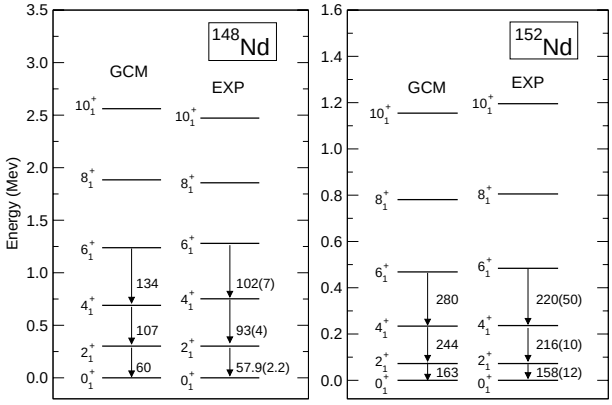

Fig. 3. The particle-number projected GCM results for the excitation energies and intraband B(E2) values (in Weisskopf units) of the ground-state bands of ^{148}Nd (left) and ^{152}Nd (right), are shown in comparison with the data (22; 23). The theoretical spectra are normalized to the experimental energies of the state 2_1^+.

^{152}Nd. Of particular interest here is the PEC of ^{150}Nd which exhibits a wide flat minimum on the prolate side ($\gamma = 0°$), with an additional miminum at $\approx$ 1.8 MeV excitation energy and oblate ($\gamma = 60°$) deformation. The two minima are separated by a potential barrier of $\approx$ 4.5 MeV. We notice the similarity between the PEC of ^{150}Nd shown in Fig. 1, and the projections on the $\gamma = 0°$ (prolate) and $\gamma = 60°$ (oblate) axes of the original X(5) potential considered by Iachello in Ref. (2) (square well in the variable β, and harmonic oscillator potential in γ). In Ref. (17) the X(5) solution has been generalized to the transition between X(5) and the rigid-rotor limit by considering an infinite square well over a confined range of values $\beta_M > \beta_m \geq 0$ (confined β-soft potential).

Correlation effects related to the restoration of broken symmetries and to fluctuations of collective coordinates are taken into account by performing configuration mixing calculations of projected states. For ^{150}Nd we have thus solved the GCM Hill-Wheller equations in the basis of constrained mean-field + LN BCS Slater determinants, projected on angular momentum and particle number. The GCM results for the two lowest bands are compared in Fig. 2 with the available data (18), and with the X(5)-symmetry predictions for the excitation energies, intraband B(E2) values (in Weisskopf units) of the ground-state ($s = 1$) and β_1 ($s = 2$) bands, and interband transitions between the ($s = 2$) and ($s = 1$) bands. To facilitate the comparison with the X(5) spectrum, which corresponds to the solution around $\gamma = 0^\circ$ (2), the GCM results in Fig. 2 have been obtained by performing configuration mixing calculations only on the prolate side (positive values of the quadrupole moment in Fig. 1). The theoretical spectra are normalized to the experimental energy of the state 2_1^+ and, in addition, the X(5) transition strengths are normalized to the experimental B(E2; $2_1^+ \rightarrow 0_1^+$). In the mean-field plus GCM approach the transition rates are calculated in the full configuration space using bare charges, and the BE(2) values can be directly compared with data. We note the excellent agreement of the GCM spectrum both with the data and with the X(5)-symmetry predictions.

When the additional mixing with oblate ($\gamma = 60^\circ$) configurations is allowed in the GCM spectrum of ^{150}Nd, a visible effect is obtained only for the ground state 0_1^+, which gets lowered in energy by ≈ 100 keV. The other states in the lowest two bands, and the corresponding E2 transition rates, are not affected by the mixing with $\gamma = 60^\circ$ configurations. In fact, since the basis of deformed states does not include the full range of γ-values ($0^\circ \leq \gamma \leq 60^\circ$), configuration mixing must be performed only on the prolate side in order to remain close to the phase-transitional region in which X(5) occurs. The spectrum resulting from a mixing of pure prolate ($\gamma = 0^\circ$) and oblate ($\gamma = 60^\circ$) configurations corresponds to a location on the hypotenuse of the right-angled extended Casten triangle (6; 7; 9), opposite to the side along which the X(5) transition takes place.

In order to demonstrate that the self-consistent GCM calculation based on the effective interaction PC-F1 predicts the shape phase transition precisely at the isotope ^{150}Nd, we also need to consider the results for the neighboring nuclei ^{148}Nd and ^{152}Nd. In Fig. 3 the particle-number projected GCM results for the excitation energies and B(E2) values (in Weisskopf units) of the ground-state bands of ^{148}Nd and ^{152}Nd are shown in comparison with available data (22; 23). The agreement with experiment is very good, especially for the strongly deformed ^{152}Nd, and of course we notice that the calculated bands and transition rates are nothing like the X(5) spectrum of ^{150}Nd. The phase transition is further illustrated in Fig. 4 where, for the yrast states of ^{148}Nd, ^{150}Nd and ^{152}Nd, we compare the B(E2; $L \rightarrow L - 2$) values and excitation energies calculated

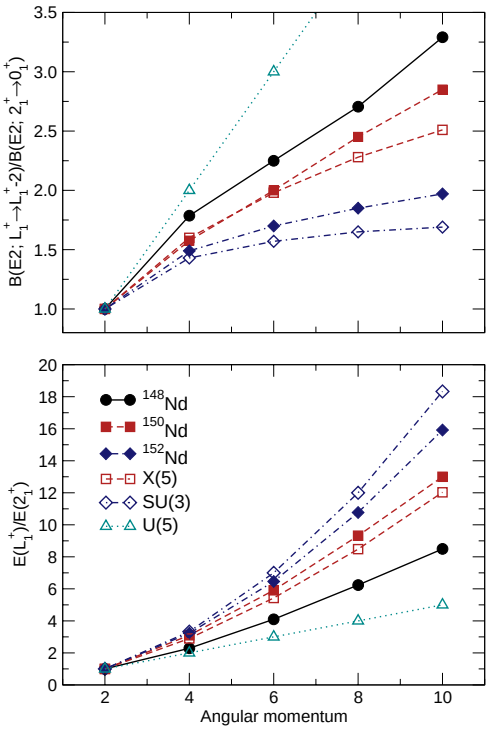

Fig. 4. B(E2; $L \rightarrow L-2$) values (upper panel) and excitation energies (lower panel) for the yrast states in ^{148}Nd, ^{150}Nd, and ^{152}Nd, calculated with the GCM and compared with those predicted by the X(5) and SU(3) symmetries (open symbols).

in the relativistic GCM model, with the corresponding values predicted by the U(5), X(5), and SU(3) symmetries. The spectrum of ^{148}Nd differs from these symmetry limits, as can already be inferred from the calculated PES in Fig. 1. The GCM E2 rates and excitation energies for ^{150}Nd closely follow those calculated from analytic expressions corresponding to the X(5) critical symmetry, whereas the yrast states of ^{152}Nd agree with the prediction of the SU(3) symmetry limit. The important result of the present analysis is that the X(5) critical symmetry, and therefore the shape phase transition, arises in the calculated spectrum of ^{150}Nd as a result of quadrupole shape fluctuations. Namely, at each point in the flat prolate minimum shown in Fig. 1, the yrast spectrum obtained by angular momentum projection from the mean-field PEC corresponds to a rotor, i.e. to the SU(3) symmetry limit. Only when quadrupole fluctuations are taken into account by GCM configuration mixing calculations, the resulting spectrum approaches the X(5) critical symmetry (Figs. 2 and 4).

3 Conclusions

In conclusion, we have demonstrated that the microscopic self-consistent mean-field framework, based on a universal energy density functional adjusted to

nuclear ground-state properties, and extended to take into account correlations related to symmetry restoration and fluctuations of collective variables, describes not only general features of shape transitions, but also the singular behavior of the excitation spectra and transition rates at the critical point of quantum shape phase transition.

References

[1] F. Iachello, Phys. Rev. Lett. 85, 3580 (2000).
[2] F. Iachello, Phys. Rev. Lett. 87, 052502 (2001).
[3] R. F. Casten and N. V. Zamfir, Phys. Rev. Lett. 85, 3584 (2000).
[4] R. F. Casten and N. V. Zamfir, Phys. Rev. Lett. 85, 052503 (2001).
[5] P. Cejnar and J. Jolie, Phys. Rev. E 61, 6237 (2000).
[6] J. Jolie, R. F. Casten, P. von Brentano, and V. Werner, Phys. Rev. Lett. 87, 162501 (2001).
[7] J. Jolie, P. Cejnar, R. F. Casten, S. Heinze, A. Linnemann, and V. Werner, Phys. Rev. Lett. 89, 182502 (2002).
[8] J. Jolie and R. F. Casten, Nucl. Phys. News. 15, 20 (2005).
[9] R. F. Casten, Nature Physics 2, 811 (2006).
[10] M. Bender, P.-H. Heenen, and P.-G. Reinhard, Rev. Mod. Phys. 75, 121 (2003).
[11] D. Vretenar, A. V. Afanasjev, G. A. Lalazissis, and P. Ring, Phys. Rep. 409, 101 (2005).
[12] J. Meng, W. Zhang, S. G. Zhou, H. Toki, and L. S. Geng, Eur. Phys. J. A 25, 23 (2005).
[13] Z.-Q. Sheng and J.-Y. Guo, Mod. Phys. Lett. A 20, 2711 (2005).
[14] R. Fossion, D. Bonatsos, and G. A. Lalazissis, Phys. Rev. C 73, 044310 (2006).
[15] T. Nikšić, D. Vretenar, and P. Ring, Phys. Rev. C 73, 034308 (2006).
[16] T. Nikšić, D. Vretenar, and P. Ring, Phys. Rev. C 74, 064309 (2006).
[17] N. Pietralla and O. M. Gorbachenko, Phys. Rev. C 70, 011304(R) (2004).
[18] R. Krücken it et al, Phys. Rev. Lett. 88, 232501 (2002).
[19] A. Leviatan, Phys. Rev. C 74, 051301(R) (2006).
[20] D. Bonatsos, D. Lenis, D. Petrellis, P. A. Terziev, and I. Yigi toglu, Phys. Lett. B 632, 238 (2006).
[21] T. Bürvenich, D. G. Madland, J. A. Maruhn, and P.-G. Reinhard, Phys. Rev. C 65, 044308 (2002).
[22] M. R. Bhat, Nucl. Data Sheets 89, 797 (2000).
[23] Agda Artna-Cohen, Nucl. Data Sheets 79, 1 (1996).